IEEE Access
Multidisciplinary | Rapid Review | Open Access Journal

Received April 29, 2021, accepted May 8, 2021, date of publication May 11, 2021, date of current version May 25, 2021.

Digital Object Identifier 10.1109/ACCESS.2021.3079171

Power-Location Optimization for Cooperative Nomadic Relay Systems Using Machine Learning Approach

HAMID AMIRIARA[1], M. REZA ZAHABI[1], AND VAHID MEGHDADI[2]
[1]Department of Electrical and Computer Engineering, Babol Noshirvani University of Technology, Babol 47148-71167, Iran
[2]XLIM UMR CNRS 7252, University of Limoges, 87032 Limoges, France

Corresponding author: Vahid Meghdadi (meghdadi@ensil.unilim.fr)

ABSTRACT The exact expressions and simple tight lower bounds for end-to-end average symbol error rate (ASER) and outage probability (OP) are derived in amplify-and-forward (AF) source-relay-destination cooperative link, provided that source-destination path is correlated with the source-relay path. Afterward, an optimum power allocation (PA) and relay location (RL) algorithm is presented. The effect of correlation factor and path-loss exponent (PLE) on the optimal nodes' power and location is investigated. The results show that optimizing relay location is more efficient than power allocation. Furthermore, a machine learning (ML) implementation of the proposed convex optimization-based algorithm is investigated to cop the computational burden. Specifically, the data set is obtained by using the proposed algorithm. Given the data set, the optimization algorithm can be translated into a regression problem, and feed-forward neural networks (FNNs) are then employed to solve this problem efficiently. The simulation results represented a compromise between accuracy and computation times for the ML-based joint PA-RL optimization.

INDEX TERMS Correlated channel, Nakagami-*m* channels, cooperative communication systems, power allocation, relay location optimization, machine learning, deep learning.

I. INTRODUCTION

Towards the Fifth Generation (5G) networks, the concept of moving networks has emerged where both devices and cells are in constant or temporary motion [1]. The requirements of the new use cases are expected to be satisfied, considering the inhomogeneous distribution of traffic over time and space [2].

Namely, the network to be deployed must react quickly and dynamically to fulfill the increased service requirements in a certain period and at a target region. In this sense, fixed small cells lack the flexibility of such networks in addition to their not-always-needed availability, which causes excess energy consumption and cost.

In this scope, one of the emerging components which enables dynamic radio topology is a movable relay, named as nomadic relay node (NRN), has been already proposed by the IEEE 802.16s Relay Task Group to serve a particular group introduced in [3] for the use in 5G. NRNs are non-operator-deployed access nodes with relay-like capabilities, which provides a complementary approach to fixed low-power Base Stations (BS), besides sharing their aforementioned advantages.

In this work, a performance evaluation of Cooperative Relays Systems (CRSs) with NRN in a downlink cellular wireless network is presented. There has been much research interest, such as [4]–[6], in examining the impact of different types of CRS's performance. However, most of the researches assumes that links are statistically independent of each other, but it is an assumption for simplicity, because in practical CRSs, wireless channels may be spatially correlated, which should be especially considered in optimizing of CRSs.

The capacity, outage behavior, and diversity gain, mainly over uncorrelated Rayleigh fading channel environments have been widely studied. Up to date, the average symbol error rate (ASER) over correlated Nakagami-*m* fading channel, has received little attention. In this context, [7] examined the performance of a Decode-and-Forward (DF) system by using the space-time orthogonality principle through Nakagami-*m* channels with integer m. In [8], we have also considered the optimization of power allocation and relay location in a CRS in the Rayleigh channel with free space path loss. In [9], the result in [8] was extended to the effect

The associate editor coordinating the review of this manuscript and approving it for publication was Francisco Rafael Marques Lima.

of path loss exponent. In [10], we also looked at the optimization of CRS in the Nakagami-*m* channel, but in [10] all the inter-nodes links were assumed to be independent and identically distributed Nakagami-*m* fading channels.

In our earlier work [8], [9], and [10], independent fading between the communication links was assumed. In contrast to earlier existing results in the literature, these links might be correlated due to common scatters or the geometry of the links in reality. For example, in [5], the performance of the DF relay system with fading correlated channels was investigated. Also, [6] examined the performance of the DF system with M-PSK modulation signals in a triple branch with a correlated Nakagami-*m* channel using the selective combination technique. The performance of a dual-hub amplify-and-forward (AF) with beamforming and spatial correlation channel was investigated in [11]. Similarly, the effects of spatial correlation within the office environment and the multi-antenna AF relay were analyzed in references [12] and [13]. In [14], the performance of the system through Rayleigh fading channels is evaluated by taking into account the correlation between S-R and R-D links, for BPSK or DPSK modulations. In addition, some authors in [15]–[17] proved the effects of spatial correlation on the performance of various relay schemes.

Many of the above research tackled the problem under the assumption of uncorrelated fading channel environments. However, in practice, a correlation exists between the source–relay and source-destination channels, e.g., for nomadic relay cooperation in the downlink of a cellular network in 5G. In addition, the optimization of resource allocation was mainly based on optimizing the performance for finding the optimal power allocation, in which the relay location might not necessarily be optimized. Also, a DF protocol for the transmission between the source and the destination through relays is considered.

According to what has been argued, this article has two goals. First, the exact expressions for the ASER and OP (Outage Probability) in an AF-CRS with NRN over the spatial correlation Nakagami-*m* channels for different modulations (such as M-ASK, M-QAM, M-PSK, etc.) are derived. In addition, simple tight bounds for ASER and OP are provided for determining the lower bounds in high SNR. The correctness of the obtained analytical results, by using computer simulations, was verified. Results show that the derived ASER and OP bounds, particularly at medium and high SNRs, are tight bounds. Second, a joint Power-Allocation Relay-Location (PA-RL) optimization algorithm is proposed based on the derived asymptotic performance expressions for finding the optimal power allocation and optimal NRN location.

While the joint PA-RL convex optimization is converted to a very compact algorithm, it might be prohibitive for operating in an in-line manner due to computational time. In the last few years, there has been a growing interest in using the machine learning approach for solving optimization problems in wireless communication, which was solved by conventional convex algorithms mostly operating in an off-line manner [18], [19]. Based on this approach, feed-forward neural networks (FNNs) are also involved in obtaining efficient computational solutions for the PA-RL optimization problem with slight compromising accuracy.

The contributions of this paper are summarized as follows:

- The exact expressions and simple tight bounds for the ASER and OP in an AF-CRS with NRN over the spatial correlation Nakagami-*m* channels for different modulations (such as M-ASK, M-QAM, M-PSK, etc.) are derived.
- The PA-RL problem is formulated for the case that a correlation exists between the links. A convex optimization-based algorithm is proposed to obtain the globally joint optimal PA-RL.
- To further reduction of computation time, the PA-RL optimization is translated into a regression problem and solved by a machine learning method, which showed a very interesting trade-off between the computation time and accuracy performance.

II. NOMADIC RELAY COOPERATION MODEL

A. COOPERATIVE NOMADIC RELAY SYSTEM

To fully exploit the capabilities of 5G, we need flexible and accessible network resources, which should be allocated dynamically to the involved users. Nomadic network, already defined as a part of 5G, is a promising technique based on dynamic resource allocation. In a nomadic network, every element of the network can move, which means that the relays, the users, and even the cells are moving. Also, some of the network elements might be mounted on the vehicle to cope with the network demands at any time and location. For instance, in a street festival, the high capacity demand of a user crowd can be met by the activation of NRNs found in the vicinity, for example, the vehicles belonging to a car-sharing company. Another example can be in the case of a road accident, where the coverage and capacity demand of the involved users can be satisfied with the police car as an NRN, arrived at the scene [2].

B. SIGNAL MODEL

Fig.1 presents CRS principles for downlink in a cellular network, with a single AF cooperative Nomadic relay. This scheme consists of a macro base station (BS), a mobile station (MS) with a single antenna, and an NRN deployed to achieve the transmit spatial diversity for link-quality improvement.

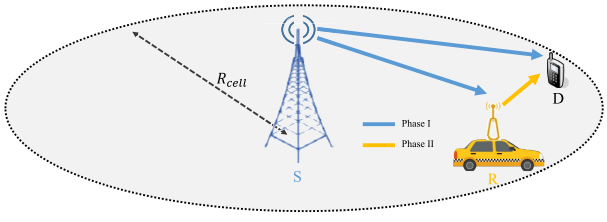

FIGURE 1. Nomadic relay node (NRN) cooperation in the downlink.

The AF cooperation protocol considered here is realized over two consecutive time slots. In the first time slot, the source "S" broadcasts the transmitted symbol to both the relay "R" and the destination "D". The relay will amplify and forward the received signal to the destination during the second time slot.

In this article, it is assumed that the maximal ratio combining (MRC) is used at the destination for combining the received signals from the first and second time slots.[1]

From the results obtained in [10], it is easy to conclude that the end-to-end instantaneous signal to noise ratio (ISNR) at the output of combiner is $\gamma_\Sigma = \gamma_0 + \gamma_1$ assuming that γ_0 and γ_1 are ISNR of S-D and S-R-D links respectively, which are defined as follows:

$$\gamma_0 = \gamma_{s,d} = \frac{P_s |h_{s,d}|^2}{N_0} \tag{1}$$

$$\gamma_1 = \frac{\frac{P_s |h_{s,r}|^2}{N_0} \times \frac{P_r |h_{r,d}|^2}{N_0}}{1 + \frac{P_s |h_{s,r}|^2}{N_0} + \frac{P_r |h_{r,d}|^2}{N_0}} \tag{2}$$

At high SNR regime (2) is often approximated by the harmonic mean as [10]

$$\gamma_1 \approx \frac{1}{\frac{1}{\gamma_{s,r}} + \frac{1}{\gamma_{r,d}}} \tag{3}$$

where $\gamma_{r,d} = \frac{P_r |h_{r,d}|^2}{N_0}$ and $\gamma_{s,r} = \frac{P_s |h_{s,r}|^2}{N_0}$ are the ISNR of R-D and S-R links, respectively; P_s and P_r are the transmitted signal power of the source and the relay, respectively; N_0 is the noise received power; $h_{s,d}$, $h_{s,r}$, and $h_{r,d}$ are the fading channel gains of the S-D, S-R, and R-D links, respectively.

C. CHANNEL MODEL

In this paper, it is assumed that the fading between the devices follows the Nakagami-m distribution, which is a general model that can easily account for both severe and moderate fading conditions. Thus, the corresponding channel power gains (i.e., $|h_{s,d}|^2$, $|h_{s,r}|^2$, and $|h_{r,d}|^2$) are the Gamma random variable [10]. Hence, the PDF of the ISNR between nodes i and j ($i, j \in \{s, r, d\}$) is Gamma density function with different parameters, i.e.,

$$\begin{aligned} f_{\gamma_{i,j}}(\gamma) &= \text{Gamma}\left(\frac{m}{\bar{\gamma}_{i,j}}, m\right) \\ &= \frac{m^m \gamma^{m-1}}{\bar{\gamma}_{i,j}^m \Gamma(m)} \exp\left(-\frac{m\gamma}{\bar{\gamma}_{i,j}}\right), \quad \gamma_{i,j} > 0 \end{aligned} \tag{4}$$

where $\bar{\gamma}_{i,j}$ is the corresponding average SNR (ASNR) values, m is the fading parameter of the Nakagami channel, whose value is determined from $1/2$ to ∞ with respect to the channel condition. For a particular case, $m = 1$, it leads to the Rayleigh model.

[1]Due to the limited space, the signal model is not shown, but details can be found in our earlier works [8], [9], or [10].

Likewise, the bivariate Gamma pdf can be expressed as

$$\begin{aligned} f(\gamma_1, \gamma_2) = &\frac{m^{m+1} (\gamma_1 \gamma_2)^{\frac{m-1}{2}}}{\Gamma(m) (\bar{\gamma}_1 \bar{\gamma}_2)^{\frac{m+1}{2}} (1-\rho) (\rho)^{\frac{m-1}{2}}} \\ &\times e^{-\frac{m\gamma_1}{(1-\rho)\bar{\gamma}_1} - \frac{m\gamma_2}{(1-\rho)\bar{\gamma}_2}} \\ &\times \mathrm{I}_{m-1}\left(\frac{2m\sqrt{\rho}}{(1-\rho)} \sqrt{\frac{\gamma_1 \gamma_2}{\bar{\gamma}_1 \bar{\gamma}_2}}\right); \quad \gamma_1, \gamma_2 \geq 0 \end{aligned} \tag{5}$$

where

$$\rho = \frac{\text{Cov}\left(|h_1|^2, |h_2|^2\right)}{\sqrt{\text{Var}\left(|h_1|^2\right) \text{Var}\left(|h_2|^2\right)}} \tag{6}$$

is the spatial correlation coefficient (SCC), Cov(.) and Var(.) are the covariance and variance operations, respectively, $\mathrm{I}_\alpha(x)$ denotes the modified Bessel function of the first kind of order α and is defined as $\sum_{k=0}^{\infty} (-1)^k / k! \Gamma(k + \alpha + 1) (x/2)^{2k+\alpha}$ [20].

III. MOMENT GENERATION FUNCTION (MGF) DERIVATION

As it can be seen from Fig. 1, the source is the BS, and the destination and the relay are the MS and the NRN, respectively. Usually, the BS is mounted high and away, and the NRN is located not very far from the MS. This indicates that the distance between the relay and the user is not very large. It is noteworthy that the optimal NRN location is on the S-D connecting line, and the R and D receive signals in the same time slot. Thus, S-D and S-R links experience approximately the same environment and are expected to be correlated. In such a case, the AF cooperation gain will decrease. As a result, in this paper, the attention is focused on the existence of a correlation between the S–D and S–R links for the Cooperative Nomadic Relay System (CNRS), with a Nakagami-m fading model.

In this section, first, an exact MGF expression and then the tight asymptotic description for MGF in high SNR values without any complex integrals or complicated special functions, e.g., the Meijer G-function and Fox H-functions is derived. The new asymptotic MGF expressions allow more manageable and more efficient analytical manipulations, which also apply to their special cases, such as the Rayleigh and Rice fading. As an illustrative application, the average symbol error rate (ASER) and outage probability (OP) for these fading models are evaluated using the new derived asymptotic MGF expressions in the next section.

A. EXACT MGF

Let ρ denote the SCC between $h_{s,d}$, and $h_{s,r}$ and considering the MGF for downlink CNRSs. Using the definition of MGF and the end-to-end ISNR $\gamma_\Sigma \approx \gamma_{s,d} + \frac{\gamma_{s,r}\gamma_{r,d}}{\gamma_{s,r}+\gamma_{r,d}}$, it is obvious that

$$\mathcal{M}_{\gamma_\Sigma}(s) = \int_0^\infty \mathrm{e}^{-sx} f_{\gamma_\Sigma}(x)\, dx$$

$$= \int_0^\infty \int_0^\infty \int_0^\infty e^{-s\gamma_{s,d} - s\frac{\gamma_{s,r}\gamma_{r,d}}{\gamma_{s,r}+\gamma_{r,d}+1}} \times f\left(\gamma_{s,d}, \gamma_{s,r}\right) f\left(\gamma_{r,d}\right) d_{\gamma_{s,d}} d_{\gamma_{s,r}} d_{\gamma_{r,d}} \quad (7)$$

By substituting (4) and (5) into (7) and performing manipulations, it can be expressed as

$$\mathcal{M}_{\gamma_\Sigma}(s) = \sum_{k=0}^{\infty} \frac{\rho^k m^{(3m+2k)} \int_0^\infty e^{\left(s+\frac{m}{(1-\rho)\bar{\gamma}_{s,d}}\right)\gamma_{s,d}} \gamma_{s,d}^{k+m-1} d\gamma_{s,d}}{k!(1-\rho)^{m+2k}\Gamma(m+k)\Gamma(m)^2\left(\bar{\gamma}_{s,d}\bar{\gamma}_{s,r}\right)^{m+k}\bar{\gamma}_{r,d}^m} \times \int_0^\infty \int_0^\infty e^{-s\frac{\gamma_{s,r}\gamma_{r,d}}{\gamma_{s,r}+\gamma_{r,d}+1}} \gamma_{s,r}^{k+m-1}\gamma_{r,d}^{m-1} \times e^{-\frac{m\gamma_{s,r}}{(1-\rho)\bar{\gamma}_{s,r}} - \frac{m\gamma_{r,d}}{(1-\rho)\bar{\gamma}_{r,d}}} d\gamma_{s,r} d\gamma_{r,d} \quad (8)$$

The 1-D integral inside the summation can straightforwardly be evaluated in the closed-form $\Gamma(k+m)/\left(s+m/(1-\rho)\bar{\gamma}_{s,d}\right)^{k+m}$. So, the MGF of the end-to-end ISNR for CNRSs over the correlated Nakagami-m fading branches can be expressed as

$$\mathcal{M}_{\gamma_\Sigma}(s) = \sum_{k=0}^{\infty} \frac{\rho^k m^{(3m+2k)} \left(s+\frac{m}{(1-\rho)\bar{\gamma}_{s,d}}\right)^{-k-m}}{k!(1-\rho)^{m+2k}\Gamma(m)^2\left(\bar{\gamma}_{s,d}\bar{\gamma}_{s,r}\right)^{m+k}\bar{\gamma}_{r,d}^m} \times \int_0^\infty \int_0^\infty e^{-s\frac{\gamma_{s,r}\gamma_{r,d}}{\gamma_{s,r}+\gamma_{r,d}+1}} \gamma_{s,r}^{k+m-1}\gamma_{r,d}^{m-1} \times e^{-\frac{m\gamma_{s,r}}{(1-\rho)\bar{\gamma}_{s,r}} - \frac{m\gamma_{r,d}}{(1-\rho)\bar{\gamma}_{r,d}}} d\gamma_{s,r} d\gamma_{r,d} \quad (9)$$

B. ASYMPTOTIC MGF

As it can be noted, equation (9) consists of a cumbersome integral, which makes it very difficult and inefficient for analytical exploitations. In this subsection, a new asymptotic MGF expression for high SNR regimes is obtained. The new expression is very accurate, and in the next section, it will be used for simple tight bounds evaluation for the ASER and OP as well as the NRN power-location optimization.

To that end, the upper bound of relay link's ISNR can be written as $\gamma_{s,r,d} = \frac{\gamma_{s,r}\gamma_{r,d}}{\gamma_{s,r}+\gamma_{r,d}+1} \leq \min\left\{\gamma_{s,r}, \gamma_{r,d}\right\}$ [21]. Therefore, the upper bound of the end-to-end ISNR of CNRS can be obtained as

$$\gamma_\Sigma \leq \min\left\{\gamma_{s,d} + \gamma_{s,r}, \gamma_{s,d} + \gamma_{r,d}\right\} \quad (10)$$

By making the necessary change of variables $\gamma' = \gamma_{s,d} + \gamma_{s,r}$ and $\gamma'' = \gamma_{s,d} + \gamma_{r,d}$, they can be readily expressed by cumulative distribution function (CDF) of the (10) as

$$F_{\gamma_\Sigma}(\gamma) = F_{\gamma'}(\gamma) + F_{\gamma''}(\gamma) - F_{\gamma'\gamma''}(\gamma, \gamma) \quad (11)$$

In the CRS, when the ISNR values for the three channels are sufficiently large or, equivalently for large $\gamma'$and γ'', the bivariate CDF of these variables will be very small ($F_{\gamma'\to\infty\gamma''\to\infty}(\gamma,\gamma) = \mathrm{P}\left\{\gamma' \leq \gamma,\ \gamma'' \leq \gamma\right\} \approx 0$), Thus, (11) is upper bounded by

$$F_{\gamma_\Sigma}(\gamma) \leq F_{\gamma_\Sigma}^{\mathrm{up}}(\gamma) = F_{\gamma'}(\gamma) + F_{\gamma''}(\gamma) \quad (12)$$

As a result, the upper bound of the PDF for the end-to-end ISNR can be computed by the derivative of (12) as

$$f_{\gamma_\Sigma}^{\mathrm{up}}(\gamma) = f_{\gamma'}(\gamma) + f_{\gamma''}(\gamma) \quad (13)$$

The $f_{\gamma'}(\gamma)$ is the PDF of two combined signals path through correlated Nakagami-m distribution [23, eq. (142)] and can be formulated as

$$f_{\gamma'}(\gamma) = \frac{\sqrt{\pi}}{\Gamma(m)}\left[\frac{m^2}{\bar{\gamma}_{s,d}\bar{\gamma}_{s,r}(1-\rho)}\right]^m \left(\frac{\gamma}{2\alpha}\right)^{m-\frac{1}{2}} \times \mathrm{I}_{m-\frac{1}{2}}\left(\alpha\gamma^2\right) e^{-\frac{m\left(\bar{\gamma}_{s,d}+\bar{\gamma}_{s,r}\right)}{2(1-\rho)\bar{\gamma}_{s,d}\bar{\gamma}_{s,r}}\gamma}; \quad \gamma \geq 0 \quad (14)$$

with $\alpha = \frac{m\left[(\bar{\gamma}_1+\bar{\gamma}_2)^2 - 4\bar{\gamma}_1\bar{\gamma}_2(1-\rho)^{1/2}\right]}{2\bar{\gamma}_1\bar{\gamma}_2(1-\rho)}$.

Since γ'' is the sum of two independent gamma-distributed random variables $\gamma'' = \gamma_{s,d} + \gamma_{r,d}$, the $f_{\gamma''}(\gamma)$ can be written as:

$$f_{\gamma''}(\gamma) = f_{\gamma_{s,d}}(\gamma) * f_{\gamma_{r,d}}(\gamma) \quad (15)$$

where $*$ is the convolution operator, and $f_{\gamma_{s,d}}(\gamma)$ and $f_{\gamma_{r,d}}(\gamma)$ denote the gamma PDF, which is in accordance with (4). Note that $f_{\gamma''}(\gamma)$ can also be obtained from (14) by putting the SCC zero ($\rho = 0$). Now the MGF of the end-to-end ISNR upper bound, according to (13) and (15), can be derived as

$$\mathcal{M}_{\gamma_\Sigma}^{\mathrm{up}}(s) = \mathcal{M}_{\gamma'}(s) + \left(\mathcal{M}_{\gamma_{s,d}}(s)\ \mathcal{M}_{\gamma_{r,d}}(s)\right) \quad (16)$$

With some manipulations, the first and the last terms can be derived according to (4), (14) as

$$\mathcal{M}_{\gamma_{i,j}}(s) = \left(1 + \frac{\bar{\gamma}_{i,j}}{m}s\right)^{-m} \quad (17)$$

$$\mathcal{M}_{\gamma'}(s) = \left(1 + \frac{\left(\bar{\gamma}_{s,d}+\bar{\gamma}_{s,r}\right)}{m}s + \frac{(1-\rho)\bar{\gamma}_{s,d}\bar{\gamma}_{s,r}}{m^2}s^2\right)^{-m} \quad (18)$$

With further simplifications, by ignoring the "one" in (17) and (18) for high SNR values, and inserting them in (16), a simple asymptotic MGF for CNRS in correlated Nakagami-m channel is obtained as

$$\mathcal{M}_{\gamma_\Sigma}^{\mathrm{up}}(s) \approx \left(\frac{(1-\rho)\bar{\gamma}_{s,d}\bar{\gamma}_{s,r}}{m^2}s^2\right)^{-m} + \left(\frac{\bar{\gamma}_{s,d}\bar{\gamma}_{r,d}}{m^2}s^2\right)^{-m} \quad (19)$$

IV. PERFORMANCE ANALYSIS

A. AVERAGE SYMBOL ERROR RATE (ASER) CALCULATION

In the following, the well-known MGF method to derive ASER for several modulations, namely MPAM, MPSK, and MQAM, is derived as

$$P_e = \frac{\alpha}{\pi}\int_0^{\frac{\pi}{2}} \mathcal{M}_{\gamma_\Sigma}\left(-\frac{g}{\sin^2\phi}\right) d\phi \quad (20)$$

where α and g are given in Table 1 [24, Ch.6].

Substituting the new simple asymptotic MGF (19) in (20), when $\rho \neq 1$, the ASER performance of CNRS over the

TABLE 1. Approximate SER for different modulations.

Modulation Type	$P_e\left(\bar{\gamma}_s\right)=\alpha Q\left(\sqrt{2g\bar{\gamma}_s}\right)$
BFSK	$P_e=Q\left(\sqrt{\bar{\gamma}_s}\right)$
BPSK	$P_e=Q\left(\sqrt{2\bar{\gamma}_s}\right)$
QPSK,4QAM	$P_e\approx 2Q\left(\sqrt{\bar{\gamma}_s}\right)$
MPAM	$P_e\approx \frac{2(M-1)}{M}Q\left(\sqrt{\frac{6\bar{\gamma}_s}{M^2-1}}\right)$
MPSK	$P_e\approx 2Q\left(\sqrt{2\bar{\gamma}_s}sin\left(\pi/M\right)\right)$
Rectangular MQAM	$P_e\approx \frac{4\left(\sqrt{M}-1\right)}{\sqrt{M}}Q\left(\sqrt{\frac{3\bar{\gamma}_s}{M-1}}\right)$
Nonrectangular MQAM	$P_e\approx 4Q\left(\sqrt{\frac{3\bar{\gamma}_s}{M-1}}\right)$

correlated channel can be approximated without evaluating the cumbersome integrals in (9) as

$$P_e^{\text{up}}=\frac{\alpha m^{2m-1}\Gamma\left(2m+\frac{1}{2}\right)}{4\sqrt{\pi}g^{2m}\Gamma\left(2m\right)}\frac{1}{\bar{\gamma}_{s,d}^m}\left(\frac{1}{(1-\rho)^m\bar{\gamma}_{s,r}^m}+\frac{1}{\bar{\gamma}_{r,d}^m}\right) \tag{21}$$

For the purpose of validating and verifying the accuracy of our derived ASER for AF-CNRS scenario, in Fig. 2, the exact ASER is compared with the proposed upper bound described by (21) in Nakagami-m spatial correlated channel with different SCC $\rho\in\{0,\ 0.1,\ 0.5,\ 0.9\}$ and with BPSK modulation (i.e., $\alpha=1$ and $g=1$). In this figure, the exact ASER is calculated numerically by inserting (9) into (20). It can be seen that the case for $m=2$ has better performance than $m=1$ as expected, because a larger value of m leads to a better channel condition. It can be also observed that when the correlation increases, CNRS with the larger values of Nakagami fading figures (m) are more vulnerable to the correlation (as expected based on (21)).

As shown in Fig. 2, there is a good match between asymptotic and exact ASER in a wide range of SNR, and for different values of the SCC. Therefore, the proposed equation (21) is appropriate for asymptotic performance analysis of the downlink communication for AF-CNRS in Nakagami-m channel with spatial correlation in the links.

B. OUTAGE PROBABILITY CALCULATION

The outage probability (P_{out}) is defined as the probability that the end-to-end ISNR falls below a given threshold value (γ_T), which can be calculated using the MGF [25, Ch.1] as follows

$$P_{\text{out}}=\mathcal{L}^{-1}\left(\frac{\mathcal{M}_{\gamma_\Sigma}(s)}{s}\right)\Big|_{\gamma_T} \tag{22}$$

where $\mathcal{L}^{-1}(.)$ denotes the inverse Laplace transform. By substituting the derived exact MGF expression (9) into (22) the exact OP is obtained as:

$$\begin{aligned}P_{\text{out}}=\mathcal{L}^{-1}(&\sum_{k=0}^{\infty}\frac{\rho^k m^{(3m+2k)}\left(s+\frac{m}{(1-\rho)\bar{\gamma}_{s,d}}\right)^{-k-m}}{k!s(1-\rho)^{m+2k}\Gamma(m)^2\left(\bar{\gamma}_{s,d}\ \bar{\gamma}_{s,r}\right)^{m+k}\bar{\gamma}_{r,d}^m}\\&\times\int_0^\infty\int_0^\infty e^{-s\frac{\gamma_{s,r}\gamma_{r,d}}{\gamma_{s,r}+\gamma_{r,d}+1}}\gamma_{s,r}^{k+m-1}\gamma_{r,d}^{m-1}\\&\times e^{-\frac{m\gamma_{s,r}}{(1-\rho)\bar{\gamma}_{s,r}}-\frac{m\gamma_{r,d}}{(1-\rho)\bar{\gamma}_{r,d}}}d\gamma_{s,r}d\gamma_{r,d})\Big|_{\gamma_0}\end{aligned} \tag{23}$$

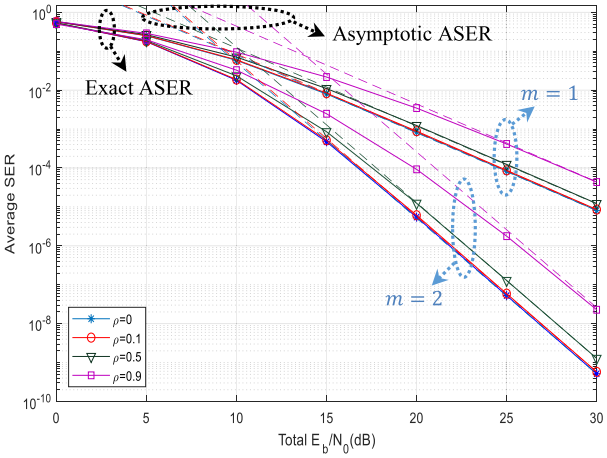

FIGURE 2. The comparison between the proposed asymptotic ASER (21), and the exact ASER by inserting (9) into (20) for the AF-CNRS with BPSK modulation. We assume that $(E|h_{s,d}|^2)=E(|h_{s,r}|^2)=E(|h_{r,d}|^2)=1$ and $P_s=P_r=1/2$ and for the channel with different values SCC and fading figures.

where the inverse Laplace transform could be performed analytically or numerically as in [25]. To avoid this mathematical complexity, the substitution of the new simple asymptotic MGF (19) in (22), under condition $\rho\neq 1$ is proposed. After some manipulations, a simple approximation of OP for CNRS over correlated channel can be derived as

$$P_{\text{out}}^{\text{up}}=\frac{\gamma_T^{2m+1}}{m^2\left(2m+1\right)!}\frac{1}{\bar{\gamma}_{s,d}^m}\left(\frac{1}{(1-\rho)^m\bar{\gamma}_{s,r}^m}+\frac{1}{\bar{\gamma}_{r,d}^m}\right) \tag{24}$$

V. JOINT POWER-LOCATION OPTIMIZATION

In the previous sections, a new asymptotic ASER and OP expressions for AF-CNRS downlink performance evaluation, which include those for M-ary modulation signals over correlated Nakagami-m fading channels was obtained. At this stage, by exploiting the proposed expressions (21) and (24), the power-location optimization problem of NRN to enhance the CNRS performance, is presented. Note that the solutions of the optimization problem are only based on partial channel state information (CSI), i.e., the Nakagami fading figure (m) and the Path Loss Exponent (PLE) (ν). Under the triangle inequality and total power constraint, the joint PA-RL optimization problem can be mathematically expressed as

$$\begin{aligned}d_{s,r}^\star,d_{r,d}^\star,P_s^\star,P_r^\star=&\underset{d_{s,r},d_{r,d},P_s,P_r}{\text{argmin}}\quad P_e\quad\text{or}\ P_{\text{out}}\\&\text{subject to: } d_{s,r}+d_{r,d}\geq d_{s,d}\\&P_s+P_r=P\end{aligned} \tag{25}$$

where $d_{s,d}$, $d_{s,r}$, and $d_{r,d}$, denote the distances of the S-D, S-R, and R-D links, respectively and P is the total normalized transmit power. In order to understand how the internode distance between nodes i and j, $d_{i,j}$, affects the overall performance, we use the wireless channel attenuation model $E\left(\left|h_{i,j}\right|^2\right)=Kd_{i,j}^{-\nu}$, $i,j\in\{s,r,d\}$, where K is a constant, that can be set to one without loss of generality. ν is the

PLE of the channel with the typical range of $2 \leq \nu \leq 8$ for the free-space environment to near ground transmission. It is clear that for the optimal solution, the relay should be placed on the connecting S-D tie line, i.e., $d_{s,r} + d_{r,d} = d_{s,d}$. Therefore, we define the distance ratio $d \triangleq d_{s,r}/d_{s,d}$, with $0 \leq d \leq 1$ and $d_{r,d} = (1-d)\, d_{s,d}$. In the same way, we define the power ratio $r \triangleq P_s/P$, with $0 \leq r \leq 1$, and $d_{r,d} = (1-d)\, d_{s,d}$. Now rewriting (21) and (24) versus d and r yields:

$$P_e(r,d) = \frac{k^2 \alpha m^{2m-1} \Gamma\left(2m+\frac{1}{2}\right) N_0^{2m} d_{s,d}^{2m}}{4\sqrt{\pi} g^{2m} \Gamma(2m) P^{2m}} \times \left(\frac{d^{m\nu}}{(1-\rho)^m r^{2m}} + \frac{(1-d)^{m\nu}}{r^m (1-r)^m}\right) \quad (26)$$

and

$$P_{\text{out}}(r,d) = \frac{\gamma_0^{2m+1} N_0^{2m} d_{s,d}^{2m}}{m^2 (2m+1)! P^{2m}} \times \left(\frac{d^{m\nu}}{(1-\rho)^m r^{2m}} + \frac{(1-d)^{m\nu}}{r^m (1-r)^m}\right). \quad (27)$$

Suppose that the MS is spatially uniformly-distributed within the cell of radius R_{cell}. The pdfs of the distance $(d_{s,d})$ and angle (θ) between the BS and the MS are expressed as $f_{d_{s,d}}\left(d_{s,d}\right) = 2d_{s,d}/R_{cell}^2$ and $f_\theta(\theta) = 1/2\pi$. Then respectively, the average ASER and OP of the MS could be calculated as

$$\begin{aligned}\bar{P}_e(r,d) &= \int_0^{2\pi}\int_0^{R_{cell}} P_e(r,d) f_{d_{s,d}}\left(d_{s,d}\right) f_\theta(\theta)\, d d_{s,d} d\theta \\ &= \frac{k^2 \alpha m^{2m-1} \Gamma\left(2m+\frac{1}{2}\right) N_0^{2m} R_{cell}^{2m}}{4(m+1)\sqrt{\pi} g^{2m} \Gamma(2m) P^{2m}} \\ &\quad \times \left(\frac{d^{m\nu}}{(1-\rho)^m r^{2m}} + \frac{(1-d)^{m\nu}}{r^m (1-r)^m}\right) \end{aligned} \quad (28)$$

and

$$\begin{aligned}&\bar{P}_{\text{out}}(r,d) \\ &= \int_0^{2\pi}\int_0^{R_{cell}} P_{\text{out}}(r,d)\ f_{d_{s,d}}\left(d_{s,d}\right) f_\theta(\theta)\, d d_{s,d} d\theta \\ &= \frac{\gamma_T^{2m+1} N_0^{2m} R_{cell}^{2m}}{m^2 (2m+1)! P^{2m}} \quad \left(\frac{d^{m\nu}}{(1-\rho)^m r^{2m}} + \frac{(1-d)^{m\nu}}{r^m (1-r)^m}\right) \end{aligned} \quad (29)$$

Note that without loss of generality, to minimize the ASER and the OP in terms of the location and power ratio, the constant factors are ignored. Therefore, the minimization problem of both ASER and OP is essentially reduced to minimize the following term:

$$\mathcal{F}(r,d) = \left(\frac{d^{m\nu}}{(1-\rho)^m r^{2m}} + \frac{(1-d)^{m\nu}}{r^m (1-r)^m}\right) \quad (30)$$

As a result, all the subsequent equations for the ASER optimization could be applied for the OP. Therefore, the joint optimization problem of (25) for both ASER and OP could be greatly simplified as

$$d^\star, r^\star = \underset{d,r\in[0,1]}{argmin}\ \mathcal{F}(r,d) \quad (31)$$

Solving the optimization problem in (31) will be performed by three steps as follows:

1) In sub-section A, the problem of the optimum relay location for the AF-CNRS, is solved.
2) In sub-section B, the optimal power allocation for the source and the relay is determined.
3) In sub-section C, the problem of joint PA-RL optimization will be presented. Then, to determine the solution of the joint optimization problem, an efficient algorithm is proposed.

A. RELAY LOCATION OPTIMIZATION

In this subsection, by adjusting the optimal location of R (i.e., d) in (30), while keeping the PA fixed (i.e., given r), the CNRS performances are optimized. The RL (Rely Location) optimization problem can be written as

$$d^\star = \underset{d\in[0,1]}{argmin}\ \mathcal{F}(r,d). \quad (32)$$

First, the convexity of this problem, i.e., the existence of a unique solution, is proved. The PLE range $2 \leq \nu \leq 8$, positive fading figure $m \geq 0$, and power ratio $0 \leq r \leq 1$, yields the positive second derivative as $\frac{\partial^2 \mathcal{F}(r,d)}{\partial d^2} = m\nu\,(m\nu-1)\left(\frac{d^{m\nu-2}}{(1-\rho)^m r^{2m}} + \frac{(1-d)^{m\nu-2}}{r^m (1-r)^m}\right)$. Thus, the optimization problem in (32), is strictly convex with respect to (w.r.t.) $d \in [0,1]$. Hence, by taking the first-order derivative of (30) w.r.t d and setting it equal to zero, the optimum distance ratio d^* can be obtained as

$$d^\star = \frac{1}{1 + \left(\frac{1-r}{(1-\rho)r}\right)^{\frac{m}{m\nu-1}}} \quad (33)$$

Consequently, the optimum S-R and R-D distances are respectively:

$$d_{s,r}^\star = d_{s,d} d^\star, \quad d_{r,d}^\star = d_{s,d}\left(1-d^\star\right) \quad (34)$$

Fig. 3 illustrates the optimal RL (i.e., $d^\star$) versus the PA (i.e., r), for different SCC ($\rho = 0,\ 0.5,\ 0.9$). According to the figure, for a fixed power ratio, one can argue that the NRN should move closer to the S when the SCC increases.

B. POWER ALLOCATION OPTIMIZATION

Likewise, the objective function of the optimal power allocation in CNRS over the correlated Nakagami-m channel by ignoring the constants can be written as

$$r^\star = \underset{r\in[0,1]}{argmin}\ \mathcal{F}(r,d). \quad (35)$$

It is not difficult to show that for $2 \leq \nu \leq 8$, $m \geq 0$, and $0 \leq d \leq 1$ the second-order derivative of (30) w.r.t. r is not negative, i.e., $\frac{\partial^2 \mathcal{F}(r,d)}{\partial r^2} \geq 0$. By the second-order

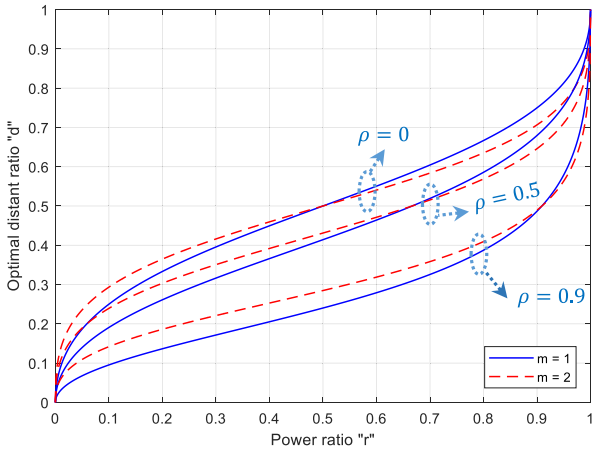

FIGURE 3. The optimal distance ratio ($d^* = d^*_{sr}/d_{sd}$), versus power ratio ($r = P_S/P$) in the AF-CNRS over correlated Nakagami-m channel with $v = 2$ and fading figure $m = 1$ (dashed line) and $m = 2$ (solid line) for the different ρ.

conditions, this indicates that (30) is convex w.r.t. r, and have a unique minimum value. Therefore, the root of its derivation with respect to r would be the optimal solution:

$$\frac{\partial \mathcal{F}(d,r)}{\partial r} = \frac{-2md^{mv}}{(1-\rho)^m r^{2m+1}} + \frac{-m(1-d)^{mv}(1-2r)}{r^{m+1}(1-r)^{m+1}} = 0 \tag{36}$$

Given that $m \neq 0$ and $r \in [0,1]$, (36) is satisfied when $2(1-r)^{m+1}d^{mv} + (1-\rho)^m(1-d)^{mv}(1-2r)\,r^m = 0$. The degree of this equation is $m+1$; that is to say, there is no explicit solution for $m > 2$, but with slight mathematical manipulation, this equation can be expressed as

$$r = 1 - \frac{1}{2 + 2(1-\rho)^{-m}\left(\frac{d}{1-d}\right)^{mv}\left(\frac{1-r}{r}\right)^m} \tag{37}$$

Now, the right-hand side of the (37) is also a function of r, and the calculation of the optimal ratio of power assignment $r^\star$ is turned to a fix-point problem $r = \mathrm{F}(r)$. The algorithm for calculating the optimal power allocation ratio $r^\star$ is presented in Algorithm 1.

In the special case when $m = 1$ (i.e., Rayleigh channel), the equation obtained from (36) will be second degree, and the optimal power ratio is readily obtained from the following closed-form equation.

$$r^\star = 1 - \frac{2}{3 + \sqrt{1 + 8\left(\frac{1}{1-\rho}\right)\left(\frac{d}{1-d}\right)^v}} \tag{38}$$

The optimum source and relay powers can be obtained as

$$P_s^\star = r^\star P, \quad P_r^\star = \left(1 - r^\star\right) P \tag{39}$$

Fig. 4 represents the optimal power ratio ($r^\star$) versus the relay distance ratios (d), for different SCCs ($\rho = 0$, 0.5, 0.9) and Nakagami fading figures ($m = 1, 2$). According to the figure, when the NRN moves to the destination (increasing d), less power is needed in the NRN

Algorithm 1 Algorithm for Calculating the Optimal Power Ratio ($r^\star$)

Input: Initial value for r (for example, $r = 0.5$), $\varepsilon = 10^{-10}$, $\mathcal{G}(r) = 1 - \frac{1}{2+2(1-\rho)^{-m}\left(\frac{d}{1-d}\right)^{mv}\left(\frac{1-r}{r}\right)^m}$

Output: $r^\star$

```
while stoping criterion has not been met do
    r_new = G(r)
    if |r_new − G(r)| ≤ ε then
        r* ← r_new
        break
    else
        r ← r_new
    end if
end while
```

(r is increased). This is because the shorter the R-D link (better communication), the overall performance of the system will depend on the S-D link. In this case, allocating more power to the source increases the CNRS performance. It is also observed that the optimal power ratio is strongly dependent on the SCC (ρ) and with increasing ρ more power must be allocated to S.

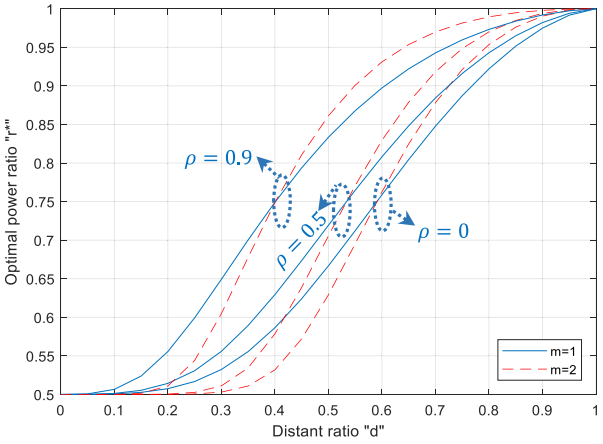

FIGURE 4. The optimal power ratio ($r^* = P^*_S/P$), versus distance ratio ($d = d_{sr}/d_{sd}$) in the AF-CRS for Nakagami channel with PLE $v = 2$. The solid line for the fading parameter $m = 1$ and the dashed line for the $m = 2$.

The proposed algorithm and (37) show that in the uncorrelated channels ($\rho = 0$) if the S-R and the R-D link are the same, i.e., $d = 1/2$, the optimal power ratio is independent of v and m and is equal to $r^* = 2/3$. It means that $P_s^* = 2/3\,P$ and $P_r^\star = 1/3\,P$, which agrees with the result obtained in [9].

C. JOINT POWER-LOCATION OPTIMIZATION

In this subsection, the problem of joint optimization of PA-RL for the source and the relay, which results in higher performance for the CNRS at the price of more complexity, is carried out. Without loss of generality, the joint power-location optimization problem (the convexity of the problem is proved

in the Appendix) can be solved in two steps, so that it can mathematically be expressed as

$$d^{\star}, r^{\star} = \underset{r\in[0,1]}{argmin}\left(\underset{d\in[0,1]}{argmin}\,\bar{P}_e\,(r,d)\right). \tag{40}$$

By inserting the optimal distance ratio $d^{\star}$, which is obtained by using (33) in the power optimization algorithm (of Algorithm 1), the optimization problem in (40) can be solved iteratively. This leads to a so-called fixed-point algorithm [26],which is shown in Algorithm 2.

For the special case of Rayleigh channel ($m = 1$), the joint optimal PA-RL can be obtained by inserting (38) in (33) that yield the following expression:

$$d = \frac{1}{1+\left(\frac{2}{1+\sqrt{1+8\left(\frac{1}{1-\rho}\right)\left(\frac{d}{1-d}\right)^{\nu}}}\right)^{\frac{1}{\nu-1}}} \tag{41}$$

This is an explicit equation versus d where fixed-point theory [9] can be used to find the optimum relay distance ratio d^*. Then the optimal power ratio (r^*) can be obtained by putting the d^* in (38) for the optimization problem.

VI. MACHINE LEARNING BASED APPROACHES

The convex optimization-based algorithm (Algorithm 2) may not be practical for time-sensitive scenarios. Therefore, we investigate an efficient computational solution based on machine learning approaches. For NRN, continuous movements will cause too many channel features changes (i.e., m, ν, ρ). Thus, we need to compute the optimal ratio (i.e., d^*, r^*). So, the machine learning input data set is $\mathbf{x} = \{m, \nu, \rho\}$, $m \in [0.5, \infty]$, $\nu \in [2, 8]$, $\rho \in [0, 1]$, and the output parameter is $\mathbf{y} = \{d^*, r^*\}$, $d \in [0, 1]$, $r \in [0, 1]$. Running the basic algorithm many times with randomly selected input arguments yield the corresponding outputs. Then the algorithm is regarded as a regression problem in the framework of the machine learning approach.

Algorithm 2 The Joint Power-Location Optimization Algorithm

Input: Initial value for r (for example, $r = 0.5$), $\varepsilon = 10^{-10}$, $\mathcal{H}(d) = 1 - \frac{1/2}{1+\left(\frac{d}{1-d}\right)}$

Output: $r^{\star}$, $d^{\star}$

```
while stoping criterion has not been met do
    d = 1 / (1+((1-r)/((1-ρ)r))^(m/(mν-1)))
    r_new = H(d)
    if |r_new − H(d)| ≤ ε then
        r* ← r_new
        d* ← d
        break
    else
        r ← r_new
    end if
end while
```

A. DATA INFORMATION

1) DATA GENERATION

A base station is assumed in the center of the unit radius cell, and MS is deployed randomly and uniformly in the cell. We assumed N as the total number of generated samples. In each run, the channel features vector (i.e., $\mathbf{x}$) is determined as input, and the optimal ratio vector (i.e., $\mathbf{y}$) calculated by using Algorithm 2 as output.

2) DATA SPLITTING

The above mentioned generated data are split into the data training (70%), the data evaluation (20%) to detect the overfitting problem and to avoid it as much as possible, the data testing (10%) to examine the performance of the neural network.

B. MACHINE LEARNING TOOL

Among the variety of machine learning approaches found in the literature, which are suitable for our regression problem, some candidates are selected, and then, by further consideration, finally FNNs are adopted for this work. A detailed consideration of neural network structures is not addressed here and is beyond the scope of this work. The configuration of FNNs is also determined by doing a trial and error procedures and taking into consideration of the input size. The neural networks used in this paper have 2 and 3 hidden layers with ([20, 10], [10, 10, 10], [20, 20, 20]) neurons, loss function mean squared error (MSE), optimizer Levenberg-Marquardt method, and epoch: 300. The Block diagram of neural network training used in this paper is depicted in Fig. 5.

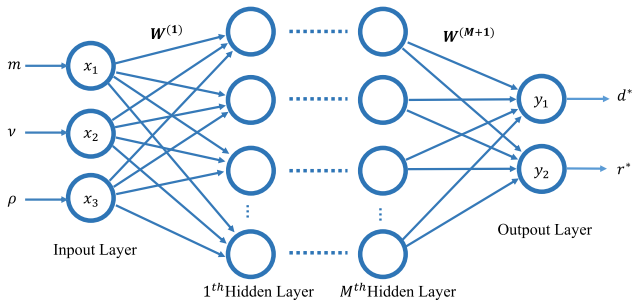

FIGURE 5. Block diagram of FNNs model used in this paper.

C. BENCHMARK

In order to provide comprehensive observations of models' predictive results, the complement of the mean absolute percentage error (MAPE) is defined as the prediction accuracy. More specifically, assuming that the number of samples is N, the accuracy is formulated as follows.

$$Accuracy = 1 - \left(\frac{100\%}{N}\sum\left|\frac{y-\bar{y}}{y}\right|\right) \tag{42}$$

VII. SIMULATION RESULT

In this section, the results of some simulations to validate the proposed equations and algorithms, are presented. In the following, the normalized noise variance (i.e., $N_0 = 1$) and normalized cell radius, i.e., $R_{cell} = 1$ are considered. Also, BPSK modulation is used, so, based on Table 1, $\alpha = 1$ and $g = 1$. In all figures, solid line and dashed lines represent the result for $\rho = 0.9$ and $\rho = 0$ respectively.

Fig. 6 shows the effect of RL on the ASER when the relay location is at the mid-point, and when it is optimized using (33). In this figure, the curves are plotted versus r for different total transmit normalized-powers, e.g. $P = P_s + P_r = \{20,\ 30,\ 40\}$dBW. Here the PLE is set to $\nu = 3$. It can be seen from Fig. 6 that the performance of an AF-CNRS with optimal relay location is superior to the system where the relay is located at mid-point. Also, the system performance is improved with the increase of total power. In addition, it can be seen that the performance improvement at an optimal location, especially at a low power ratio in correlated channel environments, is more significant. In this case, PA optimization has the largest effect on the performance improvement as the correlation increases, and with the optimization of relay location, the performance of the system in correlated channel approach to non-correlated environments.

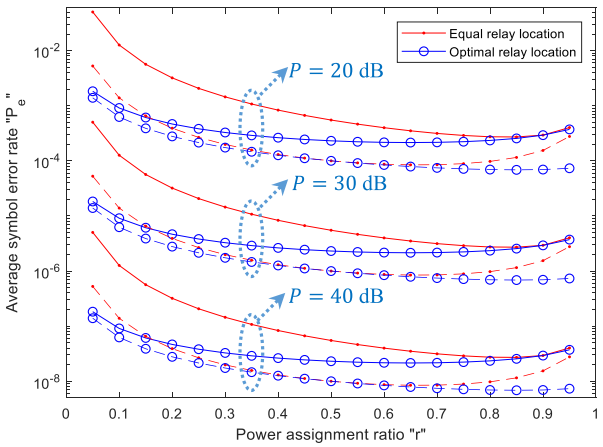

FIGURE 6. Optimum relay location in AF-CRS versus $r = P_s/(P_s + P_r)$ based on the ASER in the Nakagami channel with. For comparison, SER for a relay located at mid-point is also depicted. Solid line $\rho = 0.9$ and dashed line $\rho = 0$.

Fig. 7 depicts the ASER with equal and optimal power allocation when the total transmits normalized powers are in $P = \{20,\ 30,\ 40\}$dBW. This figure shows the performance of optimum power allocation for a given relay node location. For comparison, the performance of equal power allocation is also depicted. As seen in this figure, when the relay node is close to the destination, the power allocation strategy is more critical. Conversely, when the relay node is close to the source ($d \to 0$), equal power allocation is almost optimum ($r^* = 0.5$). Note that these conclusions are entirely consistent with the analytical results in (37). From Fig. 7, the SCC has

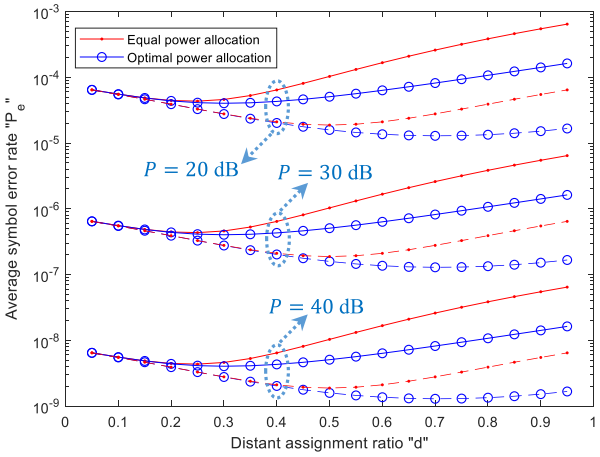

FIGURE 7. Average symbol error rate for various distance ratios, $d = d_{sr}/(d_{sr} + d_{rd})$: Optimal power allocation (blue) and equal power allocation (red) ($\nu = 3$, $m = 1$). Solid line $\rho = 0.9$ and dashed line $\rho = 0$.

a minimal effect on the performance for a small value of distance ratio ($\gamma_{s,r} \gg \gamma_{r,d}$). This result can be explained as follows: When the relay is close to the source (i.e., $d \to 0$), based on (10), the end-to-end SNR is dominated by the R-D link ($\gamma_\Sigma \approx \gamma_{r,d}$) for which no correlation is assumed. Vice versa, in cases where the relay is close to the destination (i.e., $d \to 1$), the overall SNR depends on the two correlated links, S-D, and S-R ($\gamma_\Sigma \approx \gamma_{s,d} + \gamma_{s,r}$).

Note that the joint optimization algorithm (Algorithm 2) yields a unified solution for the optimal PA and RL in AF-CNRS. First, the convergence behavior of the proposed algorithm is examined. In Fig. 8, the d^* and r^* are drawn as a function of the number of iterations and for several SCC ($\rho = 0,\ 0.5,\ 0.9$). This figure reveals that the algorithm converges very fast for all the correlation values.

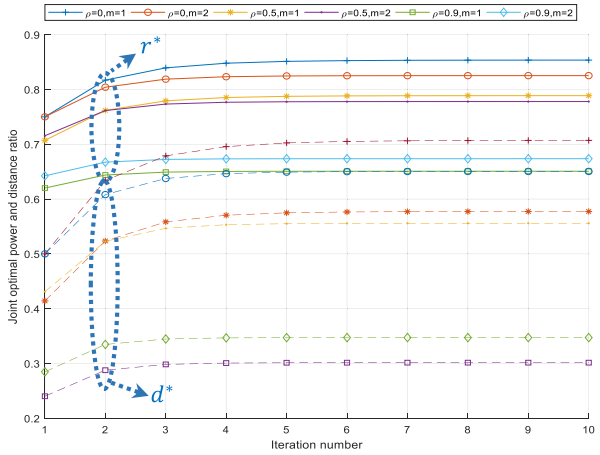

FIGURE 8. The convergence behavior of the joint power-location optimization algorithm (Algorithm 2) for $\rho = 0,\ 0.5,\ 0.9$, and $m = 1,\ 2$.

Fig. 9 presents the ASER for downlink AF-CNRS in the Nakagami channel using an asymptotic approximation

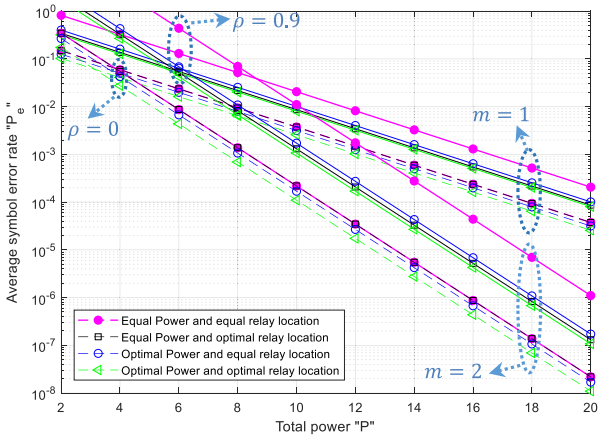

FIGURE 9. The ASER versus total power in AF cooperative: (a) $r = 0.5$, $d = 0.5$ (b) $r = 0.5$, $d = d^{\star}$ (c) $r = r^{\star}$, $d = 0.5$ (d) $r = r^{\star}$, $d = d^{\star}$. Assuming the $\nu = 3$, $m = 0.5,\ 1,\ 2$, and $\rho = 0,\ 0.9$.

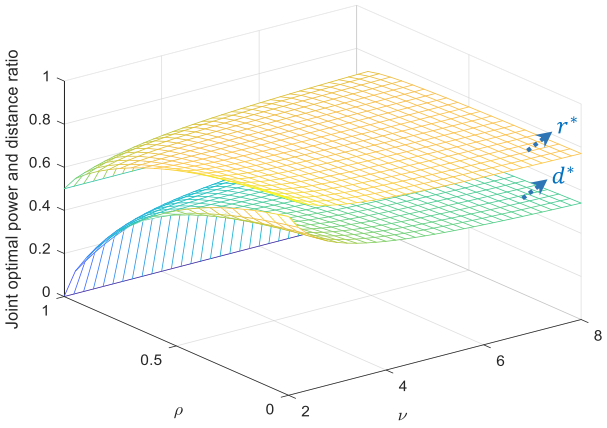

FIGURE 10. The optimal power ratio ($r^{\star}$) and optimal distance ratio ($d^{\star}$) of the AF-CNRS in a correlated Nakagami channel with $m = 1$.

in (21) as a function of the total system power with different Nakagami fading figures ($m = 0.5,\ 1, 2$) when the S-R and S-D links are correlated. To demonstrate the achievements of the proposed optimization algorithms, four scenarios are considered in Fig. 9: **a-** equal power allocation (i.e., $r = 0.5$) with the mid-point relay node (i.e., $d = 0.5$); **b-** equal power allocation (i.e., $r = 0.5$) and optimal relay node location (i.e., $d = d^{\star}$); **c-** optimal power allocation ($r = r^{\star}$) with the mid-point relay node (i.e., $d = 0.5$); and finally **d-** joint PA-RL optimum (i.e., $r = r^{\star},\ d = d^{\star}$). In case of **d** when the power allocation and relay location are jointly optimized, the ASER is further improved. Note that in the uncorrelated channel (i.e., $\rho = 0$), the performance in scenarios (**a**) and (**b**) are similar due to the fact that with equal power allocation (i.e., $r = 0.5$), the mid-point relay node is optimal (i.e., $d^{\star} = 0.5$) based on (33).

As it can be seen from Figure, the optimized RL, ASER curves are significantly superior to equal power allocation with the mid-point relay node. Furthermore, PA optimization reduces the ASER. When the PA-RL are jointly optimized, the ASER performance can be further improved. By studying the effect of SCC in Fig. 9, it is important to note that performance improvement through optimization is significantly greater when SCC increases. This improvement is negligible when ρ is small. It makes clear the importance of optimization in a correlated channel. Also, as it can be seen in the figures, the RL optimization is most effective than that of PA in correlated channel environments.

Fig. 10 illustrates the optimal power ratio ($r^{\star}$) and optimal distance ratios ($d^{\star}$) versus PLE and SCC. According to the figure, it can be argued that the relay should be placed close to the source when ρ approaches 1. That is because when the relay is close to the source ($\gamma_{s,r} > \gamma_{r,d}$), the effect of the correlation coefficient on end-to-end SNR vanishes (cf. (10)). Moreover, the figure shows that the RL ratio is more vulnerable to the correlation coefficient rather than the PA ratio, which demonstrates the importance of RL optimization in CNRSs, particularly in a correlated channel.

Here we evaluate the usefulness of machine learning in improving the implementation complexity of the optimization algorithm. The computation time of analysis was performed in order to compare the time efficiency of the convex optimization algorithm (Algorithms 2) and machine learning methods. The overall measurement results are summarized in Table 2. All the measurements were carried out at the same computer (i5-2450M CPU, Nvidia Geforce GT 620M). From this table, it can be seen that the machine learning based approach is an effective way to improve the time efficiency of computation and provides a new perspective of optimization problem solving. Also, it is evident that the increase in the number of samples (N)/hidden layers/neurons can be contributed to provide better performance.

TABLE 2. Test performance and time consumed (sec) using algorithm 2 and machine learning methods for different number of generated samples.

Cases	Number of samples (N)	Accuracy (%)	Time (msec)
Algorithm 2	$1e3$	100	1133
	$5e3$	100	5904
FNN (size: [20 10])	$1e3$	99.17	11.9
	$5e3$	99.49	15.5
FNN (size: [10 10 10])	$1e3$	99.44	13.2
	$5e3$	99.73	15.7
FNN (size: [20 20 20])	$1e3$	99.53	13.5
	$5e3$	99.82	17.6

VIII. CONCLUSION

In this paper, asymptotic ASER and OP expressions in CNRSs within the framework of dynamic radio topology in Nakagami-m correlated fading channel are evaluated. With the new derived asymptotic expressions, first, PA with fixed RL under the total transmit power constraint, is optimized. Then, the joint PA-RL optimization problem was solved with

an iterative algorithm. Finally, the optimization problem is converted to regression problems and solved by machine learning methods. The results demonstrate that machine learning based methods are useful to improving time efficiency without compromising much prediction accuracy. The results of this study confirm the utilization of CNRSs as a promising enhancement to HetNets by enabling flexible, demand-driven, and dynamic networks that are envisioned by 5G systems.

APPENDIX
PROOF OF CONVEXITY OF (30)

The Hessian matrix of $\mathcal{F}(r,d)$ is obtained as

$$\mathbf{H} = \begin{bmatrix} \dfrac{\partial^2 \mathcal{F}(r,d)}{\partial d^2} & \dfrac{\partial^2 \mathcal{F}(r,d)}{\partial d \partial r} \\ \dfrac{\partial^2 \mathcal{F}(r,d)}{\partial r \partial d} & \dfrac{\partial^2 \mathcal{F}(r,d)}{\partial r^2} \end{bmatrix},$$

where

$$\frac{\partial^2 \mathcal{F}(r,d)}{\partial d^2} = m\nu(\nu-1)\left(\frac{d^{m\nu-2}}{(1-\rho)^m r^{2m}} + \frac{(1-d)^{m\nu-2}}{r^m (1-r)^m}\right) \tag{43}$$

$$\begin{aligned}\frac{\partial^2 \mathcal{F}(r,d)}{\partial r \partial d} &= \frac{\partial^2 \mathcal{F}(r,d)}{\partial d \partial r} \\ &= \frac{-2m^2\nu d^{m\nu-1}}{(1-\rho)^m r^{2m+1}} + \frac{m^2\nu(1-d)^{m\nu-1}(1-r)}{r^{m+1}(1-r)^{m+1}}\end{aligned} \tag{44}$$

and

$$\begin{aligned}\frac{\partial^2 \mathcal{F}(r,d)}{\partial r^2} = &\frac{2m(2m+1)d^{m\nu}}{(1-\rho)^m r^{2m+2}} + \frac{2m(1-d)^{m\nu}}{r^{m+1}(1-r)^{m+1}} \\ &+ \frac{m(m+1)(1-d)^{m\nu}(1-2r)^2}{r^{m+2}(1-r)^{m+2}}\end{aligned} \tag{45}$$

It is clear that for $d, r \in [0,1]$, $\frac{\partial^2 \mathcal{F}(r,d)}{\partial d^2}$, and $\frac{\partial^2 \mathcal{F}(r,d)}{\partial r^2}$ are positive. The determinant of the $\mathbf{H}$ can be given by:

$$\begin{aligned}\det[\mathbf{H}] = &\left(\frac{\partial^2 \mathcal{F}(r,d)}{\partial d^2} \times \frac{\partial^2 \mathcal{F}(r,d)}{\partial r^2}\right) \\ &- \left(\frac{\partial^2 \mathcal{F}(r,d)}{\partial r \partial d} \times \frac{\partial^2 \mathcal{F}(r,d)}{\partial d \partial r}\right)\end{aligned} \tag{46}$$

It can be seen that (46) is nonnegative for $d, r \in [0,1]$. According to the Sylvester criterion, (30) can be proven to be convex.

REFERENCES

[1] L. Zhang, H. Zhao, S. Hou, Z. Zhao, H. Xu, X. Wu, Q. Wu, and R. Zhang, "A survey on 5G millimeter wave communications for UAV-assisted wireless networks," *IEEE Access*, vol. 7, pp. 117460–117504, 2019.
[2] *NGMN 5G White Paper*, NGMN Alliance 5G Initiative Team, NGMN, Frankfurt, Germany, 2015.
[3] C. Yang, J. Xiao, J. Li, X. Shao, A. Anpalagan, Q. Ni, and M. Guizani, "DISCO: Interference-aware distributed cooperation with incentive mechanism for 5G heterogeneous ultra-dense networks," *IEEE Commun. Mag.*, vol. 56, no. 7, pp. 198–204, Jul. 2018.
[4] S. Li, K. Yang, M. Zhou, J. Wu, L. Song, Y. Li, and H. Li, "Full-duplex amplify-and-forward relaying: Power and location optimization," *IEEE Trans. Veh. Technol.*, vol. 66, no. 9, pp. 8458–8468, Sep. 2017.
[5] A. S. J. Abdelmonem, M. Galeev, K. Komoravolu, Z. Wang, and G. Reichard, "Method and apparatus for increasing performance of communication links of cooperative communication nodes," U.S. Patent 10 039 061, Jul. 31, 2018.
[6] K. Ho-Van, P. C. Sofotasios, and S. Freear, "Underlay cooperative cognitive networks, with imperfect Nakagami-*m* fading channel information and strict transmit power constraint," *J. Commun. Netw.*, vol. 16, no. 1, pp. 10–17, Feb. 2014.
[7] K. Yang, J. Yang, J. Wu, C. Xing, and Y. Zhou, "Performance analysis of DF cooperative diversity system with OSTBC over spatially correlated Nakagami-*m* fading channels," *IEEE Trans. Veh. Technol.*, vol. 63, no. 3, pp. 1270–1281, Mar. 2014.
[8] A. Sheikvisi, H. Amiriara, and M. R. Zahabi, "Optimization of relay assignment and relay location in the cooperative wireless relay," in *Proc. Int. Conf. Res. Elect. Eng., Mech., Mechatronics*, 4th ed. Shahr, Iran: Malek Ashtar Univ. Technology, 2017, pp. 745–755.
[9] H. A. Ara, M. R. Zahabi, and V. Meghdadi, "Joint power and location optimization of relay for amplify-and-forward cooperative relaying," in *Proc. Int. Conf. Internet Things, Embedded Syst. Commun. (IINTEC)*, Dec. 2018, pp. 97–102.
[10] H. A. Ara, M. R. Zahabi, and V. Meghdadi, "Joint power-location optimization in AF cooperative relay systems with Nakagami-*m* channel," *Phys. Commun.*, vol. 40, Jun. 2020, Art. no. 101067.
[11] R. H. Y. Louie, Y. Li, H. A. Suraweera, and B. Vucetic, "Performance analysis of beamforming in two hop amplify and forward relay networks with antenna correlation," *IEEE Trans. Wireless Commun.*, vol. 8, no. 6, pp. 3132–3141, Jun. 2009.
[12] D. Liqin, W. Yang, Z. Jiliang, L. Limei, L. Xi, and Y. Dayong, "Investigation of spatial correlation for two-user cooperative communication in indoor office environment," in *Proc. IEEE 12th Int. Conf. Commun. Technol.*, Nov. 2010, pp. 420–423.
[13] T. Q. Duong, H. A. Suraweera, T. A. Tsiftsis, H.-J. Zepernick, and A. Nallanathan, "OSTBC transmission in MIMO AF relay systems with keyhole and spatial correlation effects," in *Proc. IEEE Int. Conf. Commun. (ICC)*, Jun. 2011, pp. 1–6.
[14] Y. A. Chau and K. Y.-T. Huang, "Performance of cooperative diversity on correlated dual-hop channels with an amplify-and-forward relay over Rayleigh fading environments," in *Proc. IEEE TENCON*, Nov. 2011, pp. 563–567.
[15] K. Yang, J. Yang, J. Wu, and C. Xing, "Performance analysis of cooperative DF relaying over correlated Nakagami-*m* fading channels," in *Proc. IEEE Int. Conf. Commun. (ICC)*, Jun. 2013, pp. 4973–4977.
[16] Y. Chen, R. Shi, and M. Long, "Performance analysis of amplify-and-forward relaying with correlated links," *IEEE Trans. Veh. Technol.*, vol. 62, no. 5, pp. 2344–2349, Jun. 2013.
[17] T. Q. Duong, G. C. Alexandropoulos, H. Zepernick, and T. A. Tsiftsis, "Orthogonal space-time block codes with CSI-assisted amplify-and-forward relaying in correlated Nakagami-*m* fading channels," *IEEE Trans. Veh. Technol.*, vol. 60, no. 3, pp. 882–889, Mar. 2011.
[18] G. Jia, Z. Yang, H.-K. Lam, J. Shi, and M. Shikh-Bahaei, "Channel assignment in uplink wireless communication using machine learning approach," *IEEE Commun. Lett.*, vol. 24, no. 4, pp. 787–791, Apr. 2020.
[19] D. J. S. Raj, "Machine learning based resourceful clustering with load optimization for wireless sensor networks," *J. Ubiquitous Comput. Commun. Technol.*, vol. 2, no. 1, pp. 29–38, Mar. 2020.
[20] M. Abramowitz and I. A. Stegun, *Handbook of Mathematical Functions*. New York, NY, USA: Dover, 1970.
[21] M. Hasna, "Average BER of multihop communication systems over fading channels," in *Proc. 10th IEEE Int. Conf. Electron., Circuits, Syst.*, vol. 2, Dec. 2003, pp. 723–726.
[22] M. Nakagami, "The m-distribution: A general formula of intensity distribution of rapid fading," in *Statistical Methods in Radio Wave Propagation*. Oxford, U.K.: Pergamon Press, 1960, pp. 3–36.
[23] A. Goldsmith, *Wireless Communications by Andrea Goldsmith*. Cambridge, U.K.: Cambridge Univ. Press, 2005.
[24] M. K. Simon and M.-S. Alouini, *Digital Communication Over Fading Channels*. New York, NY, USA: Wiley, 2000.

[25] J. Abate and W. Whitt, "Numerical inversion of Laplace transform of probability distribution," *ORSA J. Comput.*, vol. 7, no. 1, pp. 36–43, 1995.
[26] C. T. Kelley, *Iterative Methods for Linear and Nonlinear Equations*. Philadelphia, PA, USA: Society for Industrial and Applied Mathematics, 1995.

HAMID AMIRIARA received the B.S. degree in electronics engineering from the University of Mazandaran, Iran, in 2012, the M.S. degree (Hons.) from the Department of Electrical Engineering, Babol Noshirvani University of Technology (BNUT), Babol, Iran, in 2015, and the Ph.D. degree(Hons.) in telecommunication engineering, BNUT, in November 2020. His research interests include wireless communication, artificial intelligence, signal analysis, and relay communication. He served as a reviewer in international journals.

M. REZA ZAHABI received the B.Sc. degree from the K. N. TOOSI University of Technology, Tehran, Iran, the M.Sc. degree from the Amir Kabir University of Technology, Tehran, and the Ph.D. degree from Université de Limoges, France, in 2008, all in electrical engineering. He is currently a Faculty Member with the Babol Noshirvani University of Technology. His current research interests include wireless communication and MIMO, 5G, coding, and analog decoders.

VAHID MEGHDADI received the B.Sc. and M.Sc. degrees from the Sharif University of Technology, Tehran, Iran, in 1988 and 1991, respectively, and the Ph.D. degree from the University of Limoges, France, in 1998. He has been a Professor with the Department of Electronic and Telecommunication, ENSIL/University of Limoges, since 2000, and a Researcher with the CNRS XLIM Laboratory, Limoges, France. He served as the scientific manager for more than ten research projects in the field of Information and Communications Technology (ICT). His research interests include telecommunication systems, coding, network coding, cooperative communications, sensor networks, and massive MIMO systems.